

RSC Advances



This is an *Accepted Manuscript*, which has been through the Royal Society of Chemistry peer review process and has been accepted for publication.

Accepted Manuscripts are published online shortly after acceptance, before technical editing, formatting and proof reading. Using this free service, authors can make their results available to the community, in citable form, before we publish the edited article. This *Accepted Manuscript* will be replaced by the edited, formatted and paginated article as soon as this is available.

You can find more information about *Accepted Manuscripts* in the [Information for Authors](#).

Please note that technical editing may introduce minor changes to the text and/or graphics, which may alter content. The journal's standard [Terms & Conditions](#) and the [Ethical guidelines](#) still apply. In no event shall the Royal Society of Chemistry be held responsible for any errors or omissions in this *Accepted Manuscript* or any consequences arising from the use of any information it contains.

**Selective cell elimination in vitro and in vivo cell elimination
from tissues and tumors using antibodies conjugated with a
near infrared phthalocyanine**

Kazuhide Sato, Takahito Nakajima,

Peter L. Choyke & Hisataka Kobayashi*

Molecular Imaging Program, Center for Cancer Research, National Cancer Institute

*Corresponding author: Hisataka Kobayashi, M.D., Ph.D.

Molecular Imaging Program, Center for Cancer Research, National Cancer Institute,

NIH, Building 10, RoomB3B69, MSC1088, Bethesda, MD 20892-1088.

Phone: 301-435-4086, Fax: 301-402-3191. E-mail: Kobayash@mail.nih.gov

Abstracts

Cell cultures and tissues often contain cellular subpopulations that potentially interfere with or contaminate other cells of interest. However, it is difficult to eliminate unwanted cells without damaging the very cell population one is seeking to protect, especially established tissue. Here, we report a method of eliminating a specific subpopulation of cells from a mixed 2D or 3D cell culture *in vitro* and a mixed-population *in vivo* tumor model by using antibody-photosensitizer conjugates (APC) with a near infrared (NIR) phthalocyanine-derivative (IRdye700DX, IR700) combined with NIR light exposure with minimal damage to non-targeted cells. Thus, APC combined with NIR light exposure holds promise as method of removing specific cells from mixed cell cultures and tumors.

Introduction

For both scientific and practical reasons, elimination of a particular type of cell from a cell culture or from *in vivo* tissue is often desirable, however, it is difficult to achieve without damaging adjacent cells or the entire organism. When a cell culture is contaminated with bacteria, it is relatively straightforward to eliminate with antibiotics, however, when the contamination is with another eukaryotic cell type, selective elimination is more difficult. For example, tissue cultures based on pluripotent stem cells (PSCs), embryonic stem cells (ES), or induced pluripotent stem cell (iPS) play a key role in the field of regenerative medicine.¹⁻⁵ During tissue regeneration, a potential concern is contamination with transformed cells leading to neoplasms.⁶⁻⁹ It would be highly desirable to selectively remove these transformed cells to maintain the integrity of the tissue graft. Another example of selective cell elimination is the removal of specific immune cells from a tumor or inflammation for favorably augmenting or suppressing immune function with resulting effects on the overall growth rate of the tumor or the degree of inflammation.¹⁰ For instance, host immunity could be intentionally modulated by eliminating regulatory T cells.¹¹⁻¹⁴ Similarly, eliminating

cancer stem cells from a tumor could prevent relapse.¹⁵ Although a number of groups have investigated technologies for eliminating target cells from an established tissue or after transplantation, especially in regenerative medicine fields¹⁶⁻¹⁹, no clear practical method has been reported that does not also damage other cells in the same milieu.

The concept of using targeted light cytotoxicity using antibody-photosensitizer conjugates (APC) is over three decades old.^{20,21} Reactive oxygen species (ROS) have been implicated in the cell death associated with clinical PDT. Photon-induced redox reactions (e.g. singlet oxygen (1O_2)) caused majorly apoptosis to cell death.²² Due to the hydrophobicity of clinical photodynamic therapy (PDT) sensitizers, the pharmacokinetics of APC with PDT agents limits its selective targeting ability due to non-specific binding or uptake to normal cells or organs. The recognition that a water-soluble, near infrared (NIR) phthalocyanine-based photosensitizer (Chart 1) could be conjugated to an antibody and exposed to NIR light has led to a new method to treat tumors with light. This NIR photoimmunotherapy (NIR-PIT) differs from clinical PDT not only in the water-solubility of the photosensitizer, but also in its reliance on NIR light that has better tissue penetration than lower wavelength light. This new generation

of APC demonstrates similarly minimal non-specific binding *in vitro* and similar intravenous pharmacokinetics to naked antibodies in the body, resulting in highly targeted tumor accumulation with minimal non-target binding. When exposed to NIR light, cytotoxicity is induced only in APC-bound target cells.^{23–25}

Here, we report the feasibility of using NIR-PIT to selectively eliminate specific cells from 2D and 3D cultures or tumors.

Results and discussion

Two cell populations were used in these experiments, one tumor cell line expressing EGFR (A431) and the other control cell line, negative for EGFR (Balb/3T3). The A431 model was genetically modified to express GFP and luciferase (luc), while Balb/3T3 was modified to express RFP (Figures S1A and S1B). Specific binding of panitumumab-IR700 (Pan-IR700) to the target-expressing A431-luc-GFP cells was demonstrated, while no binding was seen in Balb/3T3-RFP cells (Figure 1A). Serial fluorescence microscopy of A431-luc-GFP cells was performed before and after PIT. After exposure to NIR light (2 J/cm^2), these cells demonstrated cellular swelling, bleb formation, rupture of the lysosome and extrusion of cellular contents (Figure 1B). PI

staining demonstrated acute cytotoxic membrane damage after PIT. These cellular changes occurred within 30 min of light exposure (Movies S1 and S2). The killing efficacy of NIR-PIT on A431-luc-GFP cells with Pan-IR700 occurred in a light-dose dependent manner as evaluated by PI staining for dead cells in 2D cell culture *in vitro* (Figures 1C and S1C). NIR-PIT also induced a decrease of luciferase-mediated bioluminescence also in a light-dose dependent manner (Figures 1D, 1E and S1D). GFP fluorescence intensity was reduced in dead cells (stained positive with PI), while GFP fluorescence was preserved in surviving cells (Figure 1F). GFP fluorescence was likely reduced after PIT because the GFP was extruded from the cytoplasm after membrane rupture and thus markedly diluted and/or denatured.²⁶ In order to investigate the change in GFP fluorescence, we compared the total GFP pixels in the same field before and after PIT (Figure 1G). The GFP fluorescence ratio decreased in a light dose dependent manner, while no decrease was detected with NIR light exposure or Pan-IR700 alone, which was confirmed by FACS analysis (Figures 1H, S1E and S1F). Collectively, these data suggested that the effects of NIR-PIT could be monitored with GFP fluorescence and luciferase activity.

Next, we evaluated the efficacy of NIR-PIT on 3D spheroids consisting of either A431-luc-GFP or Balb/3T3-RFP (Figure S2A). These cells formed spheroids as large as approximately 500 μm in diameter (Figure S2B). Three-dimensional confocal microscopy showed that these spheroids were indeed spherical (Figure S2C). Fluorescence images of frozen sections revealed that cells were evenly dispersed throughout the spheroid (Figure S2D). Pan-IR700 gradually permeated into spheroids from the perimeter as depicted on IR700-fluorescence microscopy; the stained area gradually spread toward the center of the spheroid over time (Figure S2E). NIR-PIT caused necrotic cell death in the APC-bound layer of A431-luc-GFP cells (Figure 2A and Movies S3, S4). NIR-PIT killing effects on A431-luc-GFP cells were monitored with GFP fluorescence, luciferase activity and size, all of which showed light-dose dependent responses (Figures 2B-D and S2F, S2G). Daily repeated NIR-PIT (Figures 2E and S2H) achieved complete eradication of A431-luc-GFP cells, while controls continued to grow (Figures 2F and S2I), as confirmed by GFP fluorescence, luciferase activity and size measurements (Figures 2G-I and S2J). These results suggest that repeated NIR-PIT could eradicate target-expressing cells growing in 3D spheroids.

Finally, the NIR-PIT effect was evaluated in an A431-luc-GFP flank tumor model (Figures 3 and S3A). Repeated NIR-PIT (Figure 3A) led to disappearance of both GFP signal and luciferase activity in A431-luc-GFP tumor (Figures 3B and S3A), while control tumors showed no effect (Figures 3C and 3D). *Ex vivo* A431-luc-GFP tumor images validated the *in vivo* results (Figures 3E and S3B, S3C).

In order to demonstrate selective elimination of target-expressing cells from mixed 2D and 3D cell cultures or mixed tumor models, we used the two previously described cell lines (A431-luc-GFP and Balb/3T3-RFP) (Figure S4A). Selective cell killing of A431-luc-GFP was documented with Cytox dead staining (Figure 4A). Elimination of A431-luc-GFP from an almost-confluent 2D mixed cell culture was demonstrated after NIR-PIT (Figure 4B). Repeated NIR-PIT (Figures 4C and S4B) led to complete target cell elimination without affecting the non-target cell growth (Figures 4D and S4C). Quantification of cell growth by fluorescence signal and luciferase activity confirmed the selective killing of A431-luc-GFP (Figures 4E, 4F and S4D).

With NIR-PIT, no remarkable change was detected to non-target-expressing 3D spheroid, while target 3D spheroid clearly decreased in size (Figure S5A). In order to

demonstrate target cell elimination from 3D cell culture, a mixed 3D spheroid was established (Figure S5B). Repeated NIR-PIT (Figures 5A and S5C) resulted in a decrease in size due to complete target cell elimination from the mixed 3D cell culture without damaging non-target cells (Figures 5B and S5D). Each cell population was monitored by their respective fluorescence signal or BLI, which confirmed the results (Figures 5C, 5D and S5E).

When other target cells were added to the spheroid, appropriately targeted APCs with NIR resulted in their selective elimination from 3D mixed spheroids. For instance, targeted HER2 and PSMA APCs in a mixed model of 3T3/HER2-luc-GFP and PC3-PIP-luc-GFP cells resulted in the selective elimination of the corresponding targeted cells (Figures S5F and S5G).

Finally, we demonstrated target cell elimination within a mixed tumor implanted in the flank of a mouse. As with the cell cultures, non-target-expressing tumor cells showed minimal damage, while target-expressing cells were eradicated (Figures S6A and S6B). Repeated NIR-PIT (Figure 6A) led to complete elimination of target-expressing cells from mixed tumors *in vivo* with minimal damage to non-target cells (Figures 6B and

S6C). Quantification of cell population was achieved with fluorescence signal and luciferase activity (Figures 6C and 6D). Complete cell elimination from mixed tumors was also confirmed on *ex vivo* images (Figures 6E and S6D, S6E).

In this work, we employed mixed 2D and 3D (spheroid) cell cultures, as well as a mixed tumor xenograft model *in vivo* to demonstrate selective cell elimination. Using the optical reporters, RFP, GFP and luciferase, it could be demonstrated that the selected cell population could be eliminated by NIR-PIT. Thus, we propose that NIR-PIT is a practical method for eliminating a selective set of cells from cell culture or tissue *in vitro* or local environment *in vivo* without damaging the remaining cells.

Specific cell elimination has potential application in many fields. For instance, in the field of regenerative medicine, reprogrammed PSCs have been shown to be a promising source of cells to replace damaged tissue in Parkinson's disease and age related macular degeneration.²⁷⁻²⁹ However, safety concerns arise from the formation of neoplasms during tissue formation. This can complicate the growth of replacement tissues.^{6,7} Thus, it would be of interest to selectively eliminate such cells during tissue growth or even after implantation. Similarly, in the field of immunomodulation, local elimination of

regulatory immune cells could have therapeutic consequences.^{10,30} Such diseases as rheumatoid arthritis, ankylosing spondylitis, autoimmune rheumatic disease might benefit from the local elimination of activated immune cells, resulting in decrease of inflammation.³⁰ Moreover, removing suppressing immune cells could enhance local tumor immunity.^{11–13,31–35} As a general concept, host immunity could be intentionally modulated by local elimination of specific immune cells. By careful selection of the targeting antibody, NIR–PIT could have both broad and practical utility.

Experimental

Reagents

Water soluble, silicon-phthalocyanine derivative, IRDye 700DX NHS ester was obtained from LI-COR Bioscience (Lincoln, NE, USA). Panitumumab, a fully humanized IgG₂ mAb directed against EGFR, was purchased from Amgen (Thousand Oaks, CA, USA). Trastuzumab, 95% humanized IgG₁ mAb directed against HER2, was purchased from Genentech (South San Francisco, CA, USA). All other chemicals were of reagent grade.

Synthesis of IR700-conjugated trastuzumab, panitumumab, or anti-PSMA antibody

Conjugation of dyes with mAbs was performed according to previous report.^{25,36} In brief, panitumumab, trastuzumab or anti-PSMA ab (kindly supplied by Neil Bander) (1 mg, 6.8 nmol) was incubated with IR700 NHS ester (60.2 μ g, 30.8 nmol) in 0.1 mol/L Na_2HPO_4 (pH 8.6) at room temperature for 1 hr. The mixture was purified with a Sephadex G50 column (PD-10; GE Healthcare, Piscataway, NJ, USA). The protein concentration was determined with the Coomassie Plus protein assay kit (Thermo Fisher Scientific Inc, Rockford, IL, USA) by measuring the absorption at 595 nm (8453 Value System; Agilent Technologies, Santa Clara, CA, USA). The concentration of IR700 was measured by absorption at 689 nm to confirm the number of IR700 molecules conjugated to each mAb. The synthesis was controlled so that an average of four IR700 molecules were bound to a single antibody. We performed SDS-PAGE as a quality control for each conjugate as previously reported.³⁶ The following APCs were synthesized: Trastuzumab IR700 (Tra-IR700), Panitumumab-IR700 (Pan-IR700) and antiPSMA-IR700 as PSMA-IR700.

Cell culture

GFP and luciferase stably expressed A431, 3T3/HER2 (HER2 stably expressed Balb/3T3 cells) or PC3-PIP (PSMA stably expressed PC3 cells) cells were established with a transfection of RediFect Red-FLuc-GFP (PerkinElmer, Waltham, MA, USA). High GFP and luciferase expression was confirmed with 10 passages. RFP stably expressed Balb/3T3 cells were established with transfection by RFP (EF1a)-Puro lentiviral particles (AMSBIO, Cambridge, MA, USA). High RFP expression was confirmed in the absence of a selection agent after 10 passages. We abbreviate these cells as A431-luc-GFP, 3T3/Her2-luc-GFP, PC3-PIP-luc-GFP, Balb/3T3-RFP, respectively. Cells were grown in RPMI 1640 (Life Technologies, Gaithersburg, MD, USA) supplemented with 10% fetal bovine serum and 1% penicillin/streptomycin (Life Technologies) in tissue culture flasks in a humidified incubator at 37°C at an atmosphere of 95% air and 5% carbon dioxide.

3D Spheroid culture

Spheroids were generated by the hanging drop method in which five thousand cells were suspended in 50 μ L medium and then were dispensed into 96 well plates (3D

Biomatrix Inc, Ann Arbor, MI, USA) following manufacture's instructions.²⁵ Mixed spheroids were made with 5,000 cells of Balb/3T3-RFP and 500 cells of A431-luc-GFP (100:10). After observation or treatment, spheroids were again incubated with the hanging drop plates containing new media. The volume of the spheroids was calculated with the formula: spheroid volume = $\frac{4}{3} \times \text{radius}^3$

Flow Cytometry

Fluorescence arising from the cells after incubation with APC agents was measured using a flow cytometer (FACS Calibur, BD BioSciences, San Jose, CA, USA) and CellQuest software (BD BioSciences). Cells (1×10^5) were incubated with each APC for 6 hr at 37°C. To validate the specific binding of the conjugated antibody, excess antibody (50 µg) was used to block 0.5 µg of the APC.²⁵

Fluorescence microscopy

To detect the antigen specific localization of IR700 conjugates, fluorescence microscopy was performed (IX61 or IX81; Olympus America, Melville, NY, USA). Ten thousand cells were seeded on cover-glass-bottomed dishes and incubated for 24 hr.

APC was then added to the culture medium at 10 $\mu\text{g}/\text{mL}$ and incubated at 37°C for 6 hr. The cells were then washed with PBS; Propidium Iodide (PI)(1:2000)(Life Technologies) and Cytox Blue (1:500)(Life Technologies), were used to detect dead cells. These were added to the media 30 min before observation. The cells were then exposed to NIR light and serial images were obtained. The filter was set to detect IR700 fluorescence with a 590–650 nm excitation filter, and a 665–740 nm band pass emission filter.

3D reconstructions of the spheroids were obtained with a confocal laser microscope (LSM5 meta, Carl Zeiss, Jena, Germany) after incubation for 30 min with Hoechst 33342 (1:500)(Life Technologies). Sections of spheroids were first fixed with 3.7% formaldehyde in PBS for 10 min at room temperature followed by embedding with OCT (SAKURA, Tokyo, Japan). Then, they were frozen at -80°C, cryotomed to obtain 10 μm sections (LEICA CM3050 S, Leica microsystems, Wetzlar, Germany). Analysis of the images was performed with ImageJ software (<http://rsb.info.nih.gov/ij/>).

***In vitro* NIR-PIT**

Two hundred thousand A431-luc-GFP cells were seeded into 24 well plates or twenty million cells were seeded onto a 10 cm dish and incubated for 24 hr. Medium was replaced with fresh culture medium containing 10 $\mu\text{g}/\text{mL}$ of APC which was incubated for 6 hr at 37°C. After washing with PBS, phenol red free culture medium was added. Then, cells were irradiated with a NIR LED, which emits light at 670 to 710 nm wavelength (L690-66-60; Marubeni America Co., Santa Clara, CA, USA). The actual power density (mW/cm^2) was measured with an optical power meter (PM 100, Thorlabs, Newton, NJ, USA).

Cytotoxicity/ Phototoxicity assay

The cytotoxic effects of NIR-PIT were determined bioluminescence and flow cytometric PI staining or GFP. For bioluminescence, 150 $\mu\text{g}/\text{mL}$ of D-luciferin-containing media (Gold Biotechnology, St Louis, MO, USA) was administered to PBS-washed cells 1 hr after NIR-PIT, and analyzed on a bioluminescence imaging (BLI) system (Photon Imager; Biospace Lab, Paris, France). For the flow cytometric assay, cells were trypsinized 1 hr after treatment and washed

with PBS. PI was added to the cell suspension (final 2 $\mu\text{g}/\text{mL}$) and incubated at room temperature for 30 min, prior to flow cytometry.

Estimation of GFP/RFP fluorescence intensity *in vitro*

Two hundred thousand cells were seeded on cover-glass-bottomed dishes and incubated for 12 hr. APC was then added to the culture medium (phenol red free) at 10 $\mu\text{g}/\text{mL}$ and incubated at 37°C for 6 hr. The cells were washed with PBS and media was replaced with a new, phenol red free culture medium and the under side of the cover glass was marked (to determine the position of observation). One hour after NIR-PIT, the cells were again observed. The GFP/RFP intensity was evaluated with total pixels with the same threshold in the same field of each spheroid.³⁷ Analysis of the images was performed with ImageJ software (<http://rsb.info.nih.gov/ij/>).

Fluorescence from treated cells was also measured using a flow cytometer (FACS Calibur).

Animal and tumor models

All *in vivo* procedures were conducted in compliance with the Guide for the Care and Use of Laboratory Animal Resources (1996), US National Research Council, and approved by the local Animal Care and Use Committee. Six- to eight-week-old female homozygote athymic nude mice were purchased from Charles River (NCI-Frederick). During procedures, mice were anesthetized with isoflurane.

Four million A431-luc-GFP cells were injected subcutaneously in both flanks of the mice, for the monoculture tumor model. For the mixed tumor model, mixed cells of 4×10^6 A431-luc-GFP cells and 4×10^5 Balb/3T3-RFP cells (100:10) were injected subcutaneously in the both flanks.

***In vivo* NIR-PIT**

Mice were injected with 100 μ g of Pan-IR700 and/or irradiated as follows: (1) NIR light was administered at 50 J/cm² on day 1 after injection and 100 J/cm² on day 2 to the right tumor (2) no NIR light was administered to the left tumor that served as the control and was shield. Controls included (1) only NIR light exposure at 50 J/cm² on day 1 and 100 J/cm² on day 2 to the right tumor; (2) no treatment for the left tumor.

These therapies were performed only once at day 7 after cell implantation. Mice were monitored daily, and serial image analysis was performed.

***In vivo* fluorescence imaging**

In vivo fluorescence images were obtained with a Pearl Imager (LI-COR Bioscience) for detecting IR700 fluorescence, and a Maestro Imager (CRI, Woburn, MA, USA) for GFP/ RFP. For GFP/ RFP, a band-pass filter from 445 to 490 nm (excitation) and a long-pass blue filter over 515 nm (emission) for GFP, 503 to 555 nm (excitation) and a long-pass green filter over 580 nm (emission) for RFP were respectively used. The tunable emission filter was automatically stepped in 10 nm increments from 515 to 580 nm at constant exposure (800 msec). The spectral fluorescence images consist of autofluorescence spectra and the spectra from GFP/RFP (tumor), which were then unmixed, based on the characteristic spectral pattern of GFP, using Maestro software (CRI). Regions of interest (ROIs) were manually drawn either on the flank tumor or over the abdominal region as appropriate to the model and fluorescence intensity was measured.

***In vivo* bioluminescence imaging**

For BLI, D-luciferin (15 mg/mL, 200 μ L) was injected intraperitoneally and the mice were analyzed with a Photon Imager for luciferase activity at day 6. Mice were selected for further study based on tumor size and bioluminescence. For quantifying luciferase activities, ROI of similar size were placed over the entire tumor.

Statistical Analysis

Data are expressed as means \pm s.e.m. from a minimum of four experiments, unless otherwise indicated. Statistical analyses were carried out using a statistics program (GraphPad Prism; GraphPad Software, La Jolla, CA, USA).

Conclusions

We present a method of eliminating a specific subpopulation of cells from a mixed 2D or 3D cell culture and a mixed-population *in vivo* tumor model by using the near infrared photoimmunotherapy (NIR-PIT) without damage to non-targeted cells. Using the optical reporters, RFP, GFP and luciferase, it could be demonstrated that the selected cell population could be eliminated by NIR-PIT. With this demonstration, we propose that NIR-PIT is a practical method for eliminating a selective set of cells from

cell culture or tissue in vitro or local environment in vivo without damaging the remaining cells. The directed use of light means that cells can be eliminated from only a specific region and not from the entire organism. Changing either the targeting antibodies, or the irradiated region, NIR-PIT could be an ideally generalized and feasible method of a specific cell elimination. Locally specific cell elimination by NIR-PIT has potential application in many fields, for instance, regenerative medicine, immunomodulation, and tumor immunity.

Acknowledgements

This research was supported by the Intramural Research Program of the National Institutes of Health, National Cancer Institute, Center for Cancer Research. K.S. is supported with JSPS Research Fellowship for Japanese Biomedical and Behavioral Researchers at NIH.

References

1. S. Yamanaka, *Cell Stem Cell*, 2012, **10**, 678–84.

2. M. a Birchall and A. M. Seifalian, *Lancet*, 2014, **6736**, 11–12.
3. E. Kiskinis and K. Eggan, *J. Clin. Invest.*, 2010, **120**, 51–59.
4. K. Okita, T. Ichisaka, and S. Yamanaka, *Nature*, 2007, **448**, 313–7.
5. D. a Robinton and G. Q. Daley, *Nature*, 2012, **481**, 295–305.
6. U. Ben-David and N. Benvenisty, *Nat. Rev. Cancer*, 2011, **11**, 268–77.
7. J. H. Hanna, K. Saha, and R. Jaenisch, *Cell*, 2010, **143**, 508–25.
8. I. Klimanskaya, N. Rosenthal, and R. Lanza, *Nat. Rev. Drug Discov.*, 2008, **7**, 131–42.
9. K. Ohnishi, K. Semi, T. Yamamoto, M. Shimizu, A. Tanaka, K. Mitsunaga, K. Okita, K. Osafune, Y. Arioka, T. Maeda, H. Soejima, H. Moriwaki, S. Yamanaka, K. Woltjen, and Y. Yamada, *Cell*, 2014, **156**, 663–77.
10. E. J. Wehrens, B. J. Prakken, and F. van Wijk, *Nat. Rev. Rheumatol.*, 2012, **9**, 34–42.
11. A. Marabelle and H. Kohrt, *J. Clin. Invest.*, 2013, **123**.
12. A. Marabelle, H. Kohrt, C. Caux, and R. Levy, *Clin. Cancer Res.*, 2014, **20**, 1747–56.
13. I. Mellman, G. Coukos, and G. Dranoff, *Nature*, 2011, **480**, 480–9.
14. D. M. Pardoll, *Nat. Rev. Cancer*, 2012, **12**, 252–64.
15. P. Valent, D. Bonnet, R. De Maria, T. Lapidot, M. Copland, J. V Melo, C. Chomienne, F. Ishikawa, J. J. Schuringa, G. Stassi, B. Huntly, H. Herrmann, J. Soulier, A. Roesch, G. J. Schuurhuis, S. Wöhrer, M. Arock, J. Zuber, S. Cerny-Reiterer, H. E. Johnsen, M. Andreeff, and C. Eaves, *Nat. Rev. Cancer*, 2012, **12**, 767–75.
16. U. Ben-David, N. Nudel, and N. Benvenisty, *Nat. Commun.*, 2013, **4**, 1992.

17. M.-O. Lee, S. H. Moon, H.-C. Jeong, J.-Y. Yi, T.-H. Lee, S. H. Shim, Y.-H. Rhee, S.-H. Lee, S.-J. Oh, M.-Y. Lee, M.-J. Han, Y. S. Cho, H.-M. Chung, K.-S. Kim, and H.-J. Cha, *Proc. Natl. Acad. Sci. U. S. A.*, 2013, **110**, E3281–90.
18. K. Miura, Y. Okada, T. Aoi, A. Okada, K. Takahashi, K. Okita, M. Nakagawa, M. Koyanagi, K. Tanabe, M. Ohnuki, D. Ogawa, E. Ikeda, H. Okano, and S. Yamanaka, *Nat. Biotechnol.*, 2009, **27**, 743–5.
19. C. Tang, A. S. Lee, J.-P. Volkmer, D. Sahoo, D. Nag, A. R. Mosley, M. a Inlay, R. Ardehali, S. L. Chavez, R. R. Pera, B. Behr, J. C. Wu, I. L. Weissman, and M. Drukker, *Nat. Biotechnol.*, 2011, **29**, 829–34.
20. D. Mew, C. Wat, G. H. N. Towers, and J. G. Levy, *J. Immunol.*, 1983, **130**, 1473–1477.
21. a R. Oseroff, D. Ohuoha, T. Hasan, J. C. Bommer, and M. L. Yarmush, *Proc. Natl. Acad. Sci. U. S. A.*, 1986, **83**, 8744–8.
22. P. Agostinis, K. Berg, K. a Cengel, T. H. Foster, A. W. Girotti, S. O. Gollnick, S. M. Hahn, M. R. Hamblin, A. Juzeniene, D. Kessel, M. Korbelik, J. Moan, P. Mroz, D. Nowis, J. Piette, B. C. Wilson, and J. Golab, *CA. Cancer J. Clin.*, 2011, **61**, 250–81.
23. M. Mitsunaga, M. Ogawa, N. Kosaka, L. T. Rosenblum, and P. L. Choyke, *Nat. Med.*, 2011, **17**, 1685–1691.
24. M. Mitsunaga, T. Nakajima, K. Sano, P. L. Choyke, and H. Kobayashi, *Bioconjug. Chem.*, 2012, **23**, 604–609.
25. K. Sato, R. Watanabe, H. Hanaoka, T. Harada, T. Nakajima, I. Kim, C. H. Paik, P. L. Choyke, and H. Kobayashi, *Mol. Oncol.*, 2014, **8**, 620–632.
26. K. Sato, P. L. Choyke, and H. Kobayashi, *PLoS One*, 2014, **9**, e113276.
27. M. Sundberg, H. Bogetofte, and T. Lawson, *Stem Cells*, 2013, **31**, 1548–1562.
28. H. Kamao, M. Mandai, S. Okamoto, N. Sakai, A. Suga, S. Sugita, J. Kiryu, and M. Takahashi, *Stem cell reports*, 2014, **2**, 205–18.

29. A. Morizane, D. Doi, T. Kikuchi, K. Okita, A. Hotta, T. Kawasaki, T. Hayashi, H. Onoe, T. Shiina, S. Yamanaka, and J. Takahashi, *Stem cell reports*, 2013, **1**, 283–92.
30. G. R. Burmester, E. Feist, and T. Dörner, *Nat. Rev. Rheumatol.*, 2014, **10**, 77–88.
31. Y. Bulliard, R. Jolicoeur, M. Windman, S. M. Rue, S. Ettenberg, D. a Knee, N. S. Wilson, G. Dranoff, and J. L. Brogdon, *J. Exp. Med.*, 2013, **210**, 1685–93.
32. W. H. Fridman, F. Pagès, C. Sautès-Fridman, and J. Galon, *Nat. Rev. Cancer*, 2012, **12**, 298–306.
33. J. J. O’Shea, Y. Kanno, and A. C. Chan, *Cell*, 2014, **157**, 227–40.
34. D. F. Quail and J. a Joyce, *Nat. Med.*, 2013, **19**, 1423–37.
35. T. Okazaki, S. Chikuma, Y. Iwai, S. Fagarasan, and T. Honjo, *Nat. Immunol.*, 2013, **14**, 1212–8.
36. K. Sano, T. Nakajima, P. L. Choyke, and H. Kobayashi, *ACS Nano*, 2013, **7**, 717–724.
37. K. Sato, T. Watanabe, S. Wang, M. Kakeno, K. Matsuzawa, T. Matsui, K. Yokoi, K. Murase, I. Sugiyama, M. Ozawa, and K. Kaibuchi, *Mol. Biol. Cell*, 2011, **22**, 3103–19.

Figure/ Chart legends

Chart 1

Structures of IR700.

Fig. 1

Characterization of A431 cell line and effect of NIR-PIT.

(A) A431-luc-GFP cells demonstrate EGFR expression. Specific binding was demonstrated with a blocking study. Non-EGFR expressing Balb/3T3-RFP cells were also examined with Pan-IR700 incubation, which confirmed no binding. (B) A431-luc-GFP cells were incubated with Pan-IR700 for 6 hr, and observed with a microscope before and after irradiation of NIR light (2 J/cm^2). Necrotic cell death was observed after exposure to NIR light (1 hr after PIT). Bar = 10 μm . Membrane damage and necrosis induced by NIR-PIT was confirmed by dead cell PI staining. (C) Membrane damage and necrosis induced by NIR-PIT was measured by dead cell count using PI staining on FACS. Cell killing increased in a NIR-light dose-dependent manner. Representative FACS data were presented in Figure S1C. (D) Bioluminescence in A431-luc-GFP cells was measured as relative light unit (RLU), and was decreased in a NIR-light dose-dependent manner (1 hr after PIT). Representative BLI were presented in Figure S1D. (E) BLI of a 10 cm dish demonstrated that luciferase activity in A431-luc-GFP cells decreased in a NIR-light dose-dependent manner. (F) A431-luc-GFP cells were incubated with Pan-IR700 for 6 hr and irradiated

with NIR-light (0.5 J/cm^2). GFP-fluorescence intensity decreased in dead cells (*) but was unchanged in living cells at 1 hr after NIR-PIT. Bar = $50 \mu\text{m}$. (G) Quantification of GFP-fluorescence intensity showed a decrease in a NIR-light dose-dependent manner (total pixel of GFP fluorescence in the same field)(n = 12 fields). Representative microscopic data were presented in Figure S1E. (H) GFP fluorescence intensity decreased after NIR-PIT in a NIR-light dose-dependent manner as measured by FACS. Representative FACS data were presented in Figure S1F.

Fig. 2

Characterization of 3D culture and effect of NIR-PIT.

(A) 3D spheroid at day 7 after 6hr incubation with Pan-IR700, before and 1 hr after irradiation of NIR light (2 J/cm^2). Necrotic cell death was observed 1hr after NIR light. Bar = $100 \mu\text{m}$. Regions of decreased GFP fluorescence co-localize with PI staining. (B) Day 7 3D spheroid after 6hr incubation with Pan-IR700, before and 1 day after irradiation with NIR light. Necrotic cell death was observed 1 day after NIR exposure (stained by PI). GFP-fluorescence intensity decreased and the spheroid decreased in size in a light dose dependent manner. Quantification of GFP-fluorescence demonstrated a

NIR-light dose-dependent decrease in intensity (total pixel of GFP fluorescence in the same spheroid)(n = 10). Representative microscopic data were presented in Figure S2F.

(C) Bioluminescence in A431-luc-GFP 3D spheroids decreased in a NIR-light dose-dependent manner (n = 10). Representative BLI data were presented in Figure

S2G. (D) The volume of A431-luc-GFP 3D spheroids also decreased in a NIR-light dose-dependent manner (n = 10). Representative microscopic data were presented in

Figure S2F. (E) The PIT regimen incorporating repeated NIR light exposures is shown.

(F) Day 7 A431-luc-GFP 3D spheroids were divided into 4 groups as shown (2 groups were presented in Figure S2I). Bar = 100 μ m. (G) Quantification of GFP-fluorescence

intensity showed progressive decreases after repeated NIR-PIT eventually resulting in no detectable fluorescence (total pixels of GFP fluorescence in the same spheroid)(n =

10). (H) Bioluminescence decreased progressively after repeated NIR-PIT eventually resulting in 0 (under the background level)(n = 10). Representative BLI data were

presented in Figure S2J. (I) The volume of A431-luc-GFP 3D spheroids also decreased after repeated PIT (n = 10).

Fig. 3

Characterization of in vivo NIR-PIT effect.

(A) The NIR-PIT regimen incorporating repeated NIR light exposures is shown. (B) *In vivo* GFP/ IR700 fluorescence imaging and BLI of bilateral flank tumors in response to NIR-PIT. The tumor treated with NIR-PIT demonstrated loss of GFP fluorescence and bioluminescence (Additional two mice images were in Figure S3A). (C) Quantification of GFP-fluorescence showed a progressive decrease in intensity after repeated NIR-PIT eventually resulting in complete loss of signal (n = 10 in each group). (D) Bioluminescence decreased progressively after NIR-PIT eventually resulting in complete loss of RLU (n = 10). (E) Representative image of *ex vivo* tumors showed complete eradication. Control was presented in Figure S3C.

Fig. 4**Target cell elimination in 2D cell culture.**

(A) Mixture of A431-luc-GFP cells and Balb/3T3-RFP cells were incubated with Pan-IR700 for 6 hr. Baseline and 1 hour post-NIR-PIT (2 J/cm^2) microscopic images demonstrate specific cell killing of A431-luc-GFP. Bar = 20 μm . Membrane damage

and necrosis induced by NIR-PIT was confirmed by dead cell Cyttox staining. Representative image demonstrates that A431-luc-GFP cells were eliminated 1hr after NIR-PIT. Bar = 200 μm . (B) An almost confluent mixed cell culture of A431-luc-GFP and Balb/3T3-RFP was used. Cells were incubated with Pan-IR700 for 6 hr, and observed before and after irradiation with NIR light (2 J/cm^2). (C) Repeated NIR-PIT (2 J/cm^2) regimen is shown (2 J/cm^2). (D) Repeated NIR-PIT completely eliminated targeted cells with no harm to non-targeted cells, until non-target cells became confluent. 100:10 ratio mixtures of A431-luc-GFP and Balb/3T3-RFP cells were cultured (other groups are in Figure S4C). Bar = 200 μm . (E) Quantification of fluorescence ratios showed complete elimination of targeted cells and no effect on non-targeted cells. (n = 10 fields in each group) (F) Quantification of luciferase activities (RLU ratio) demonstrates complete target cell elimination (n = 10 in each group). BLI was in Figure S4D.

Fig. 5

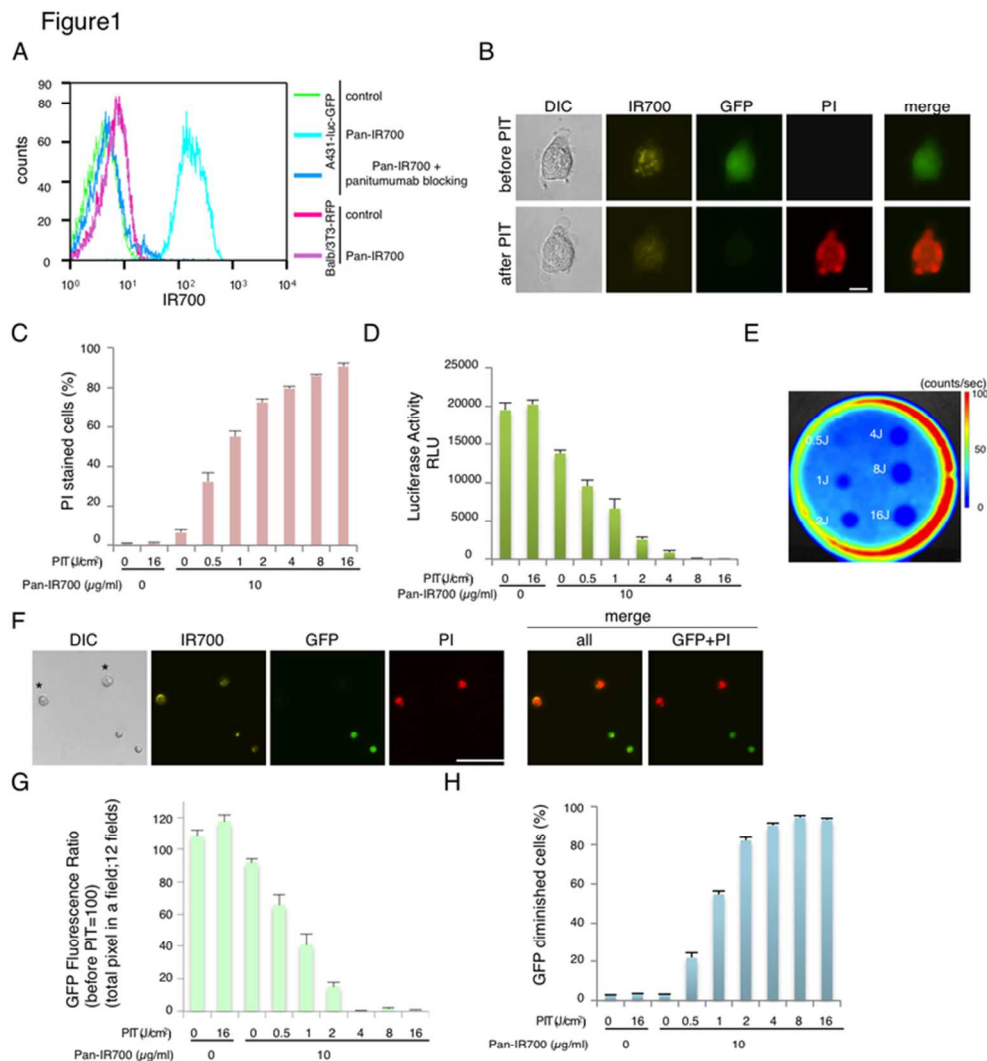
Target cell elimination in 3D cell spheroids.

(A) NIR-PIT (2 J/cm^2) regimen is shown. (B) Repeated NIR-PIT completely eliminated target cells with no harm to non-target cells, in a mixed 3D spheroid (other groups are in Figure S5D). Bar = $200 \mu\text{m}$. (C) Quantification of fluorescence ratios showed complete elimination of target cells and no effect on non-target cells. ($n = 10$ spheroids in each group) (D) Quantification of luciferase activities (RLU ratio) demonstrated complete elimination of target cells ($n = 10$ spheroids in each group). BLI and IR700 fluorescence images were in Figure S5E.

Fig. 6

Target cell elimination within a mixed tumor model *in vivo*.

(A) NIR-PIT (2 J/cm^2) regimen is shown. (B) Repeated NIR-PIT completely eliminated target cells from mixed tumors *in vivo*. (C) Quantification of fluorescence ratios showed complete elimination of target cells in mixed tumors (Additional two mice images were in Figure S6C)($n = 10$ in each group). (D) Quantification of luciferase activities (RLU ratio) demonstrated complete elimination of target cells *in vivo*. ($n = 10$ in each group). (E) Representative image of *ex vivo* tumors showed complete elimination of target cells from mixed tumors. Control was presented in Figure S6E.

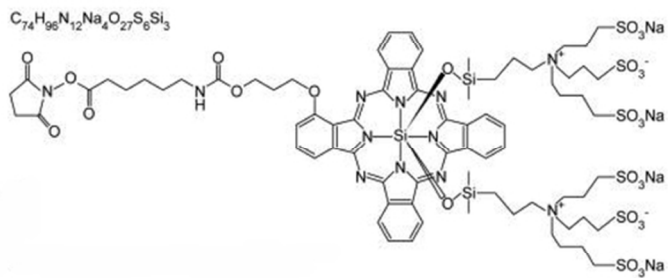


Effect of APC with NIR light to A431 cell line.

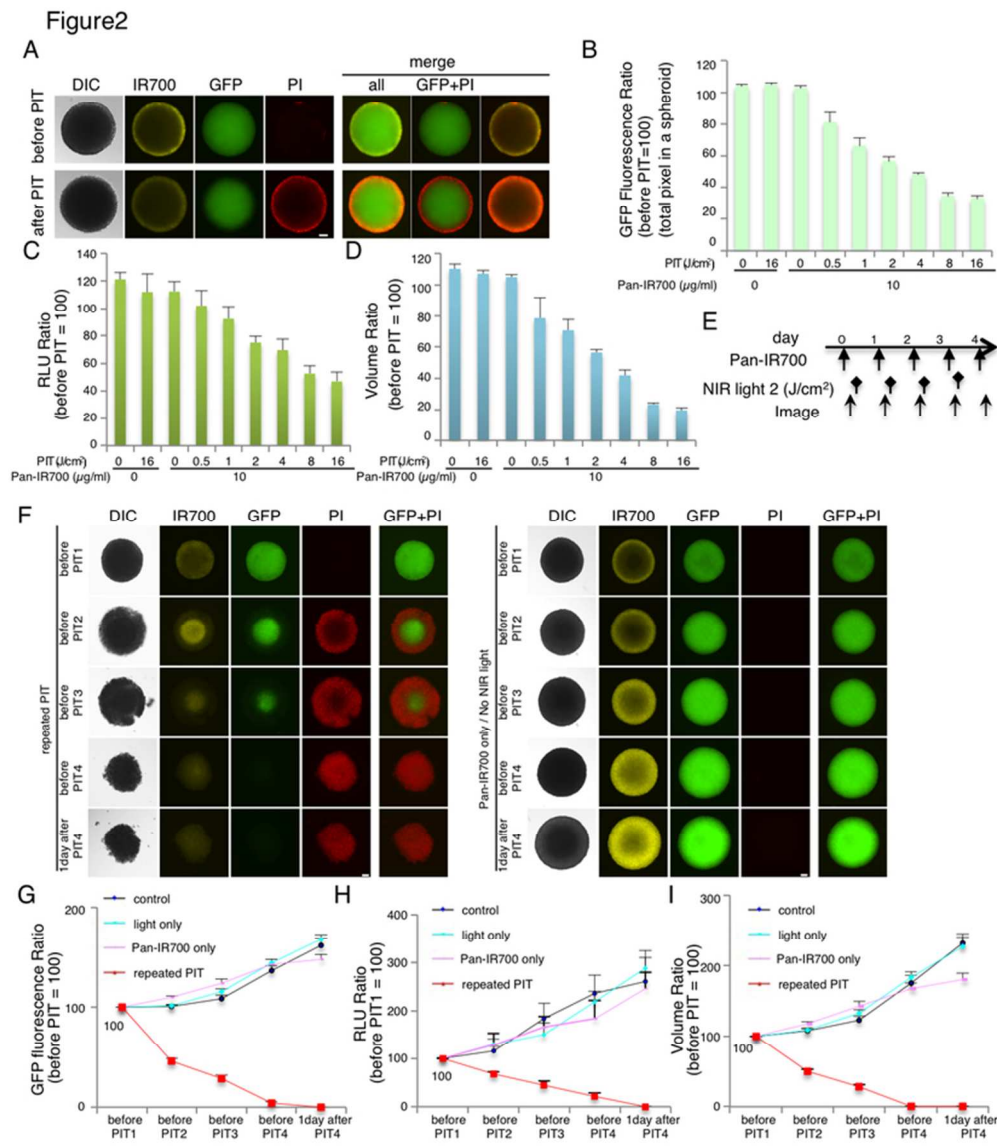
(A) A431-luc-GFP cells demonstrate EGFR expression. Specific binding was demonstrated with a blocking study. Non-EGFR expressing Balb/3T3-RFP cells were also examined with Pan-IR700 incubation, which confirmed no binding. (B) A431-luc-GFP cells were incubated with Pan-IR700 for 6 hr, and observed with a microscope before and after exposure of NIR light (2 J/cm^2). Necrotic cell death was observed after exposure to NIR light (1 hr after PIT). Bar = $10 \mu\text{m}$. Membrane damage and necrosis induced by APC with NIR light was confirmed by dead cell PI staining. (C) Membrane damage and necrosis induced by APC with NIR light was measured by dead cell count using PI staining on FACS. Cell killing increased in a NIR-light dose-dependent manner. Representative FACS data were presented in Figure S1C. (D) Bioluminescence in A431-luc-GFP cells was measured as relative light unit (RLU), and was decreased in a NIR-light dose-dependent manner (1 hr after PIT). Representative BLI were presented in Figure S1D. (E) BLI of a 10 cm dish demonstrated that luciferase activity in A431-luc-GFP cells decreased in a NIR-light dose-dependent manner. (F) A431-luc-GFP cells were incubated with Pan-IR700 for 6 hr and irradiated with NIR-light (0.5 J/cm^2). GFP-fluorescence intensity decreased in dead cells (*) but was unchanged in living cells at 1 hr after APC with NIR light exposure. Bar = $50 \mu\text{m}$. (G) Quantification of GFP-fluorescence intensity showed a

decrease in a NIR-light dose-dependent manner (total pixel of GFP fluorescence in the same field)(n = 12 fields). Representative microscopic data were presented in Figure S1E. (H) GFP fluorescence intensity decreased after APC with NIR light in a NIR-light dose-dependent manner as measured by FACS. Representative FACS data were presented in Figure S1F.
70x80mm (300 x 300 DPI)

Chart 1



Structure of a near infrared phthalocyanine (IR700).
70x80mm (300 x 300 DPI)



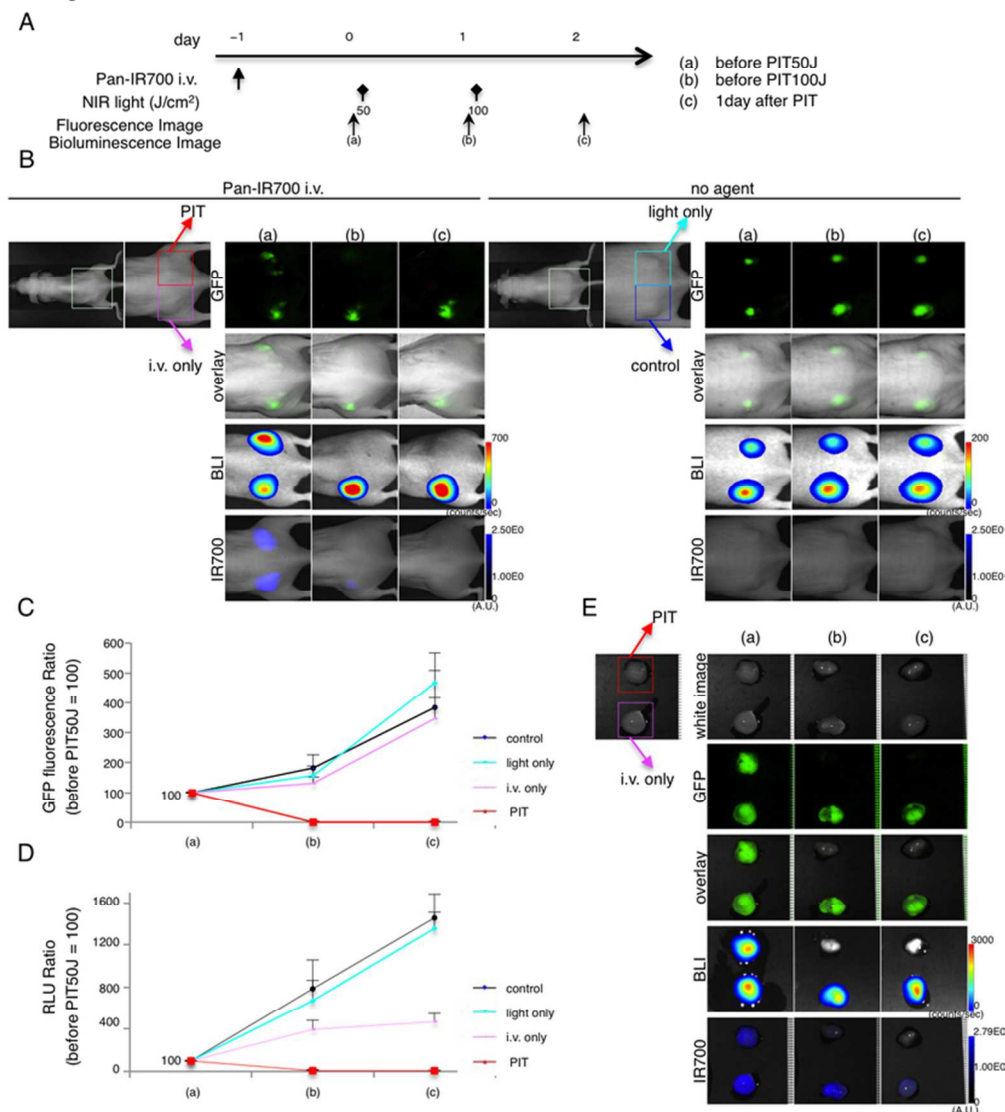
Effects of APC with NIR light to cells to 3D spheroids ex vivo.

(A) 3D spheroid at day 7 after 6hr incubation with Pan-IR700, before and 1 hr after irradiation of NIR light (2 J/cm²). Necrotic cell death was observed 1hr after NIR light. Bar = 100 µm. Regions of decreased GFP fluorescence co-localize with PI staining. (B) Day 7 3D spheroid after 6hr incubation with Pan-IR700, before and 1 day after irradiation with NIR light. Necrotic cell death was observed 1 day after NIR exposure (stained by PI). GFP-fluorescence intensity decreased and the spheroid decreased in size in a light dose dependent manner. Quantification of GFP-fluorescence demonstrated a NIR-light dose-dependent decrease in intensity (total pixel of GFP fluorescence in the same spheroid) (n = 10). Representative microscopic data were presented in Figure S2F.

(C) Bioluminescence in A431-luc-GFP 3D spheroids decreased in a NIR-light dose-dependent manner (n = 10). Representative BLI data were presented in Figure S2G. (D) The volume of A431-luc-GFP 3D spheroids also decreased in a NIR-light dose-dependent manner (n = 10). Representative microscopic data were presented in Figure S2F. (E) The PIT regimen incorporating repeated NIR light exposures is shown. (F) Day 7 A431-luc-GFP 3D spheroids were divided into 4 groups as shown (2 groups were presented in Figure S2I). Bar = 100 µm. (G) Quantification of GFP-fluorescence intensity showed progressive decreases after repeated

APC with NIR light eventually resulting in no detectable fluorescence (total pixels of GFP fluorescence in the same spheroid)(n = 10). (H) Bioluminescence decreased progressively after repeated APC with NIR light eventually resulting in 0 (under the background level)(n = 10). Representative BLI data were presented in Figure S2J. (I) The volume of A431-luc-GFP 3D spheroids also decreased after repeated PIT (n = 10).
70x80mm (300 x 300 DPI)

Figure 3

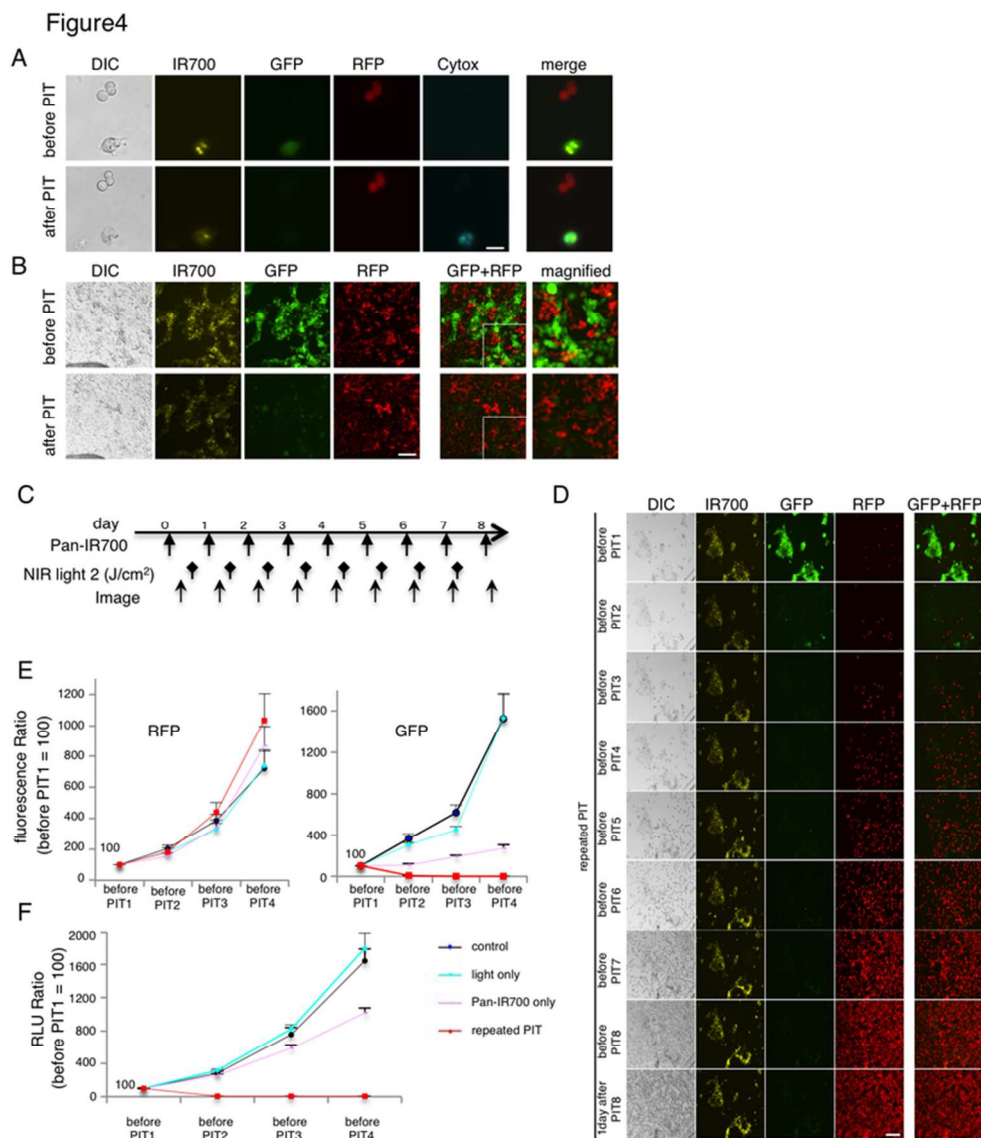


Effects of APC with NIR light to tumors in vivo.

(A) The APC with NIR light regimen incorporating repeated NIR light exposures is shown. (B) In vivo GFP/IR700 fluorescence imaging and BLI of bilateral flank tumors in response to APC with NIR light. The tumor treated with APC with NIR light demonstrated loss of GFP fluorescence and bioluminescence (Additional two mice images were in Figure S3A). (C) Quantification of GFP-fluorescence showed a progressive decrease in intensity after repeated APC with NIR light eventually resulting in complete loss of signal ($n = 10$ in each group). (D) Bioluminescence decreased progressively after APC with NIR light eventually resulting in complete loss of RLU ($n = 10$). (E) Representative image of ex vivo tumors showed complete eradication.

Control was presented in Figure S3C.

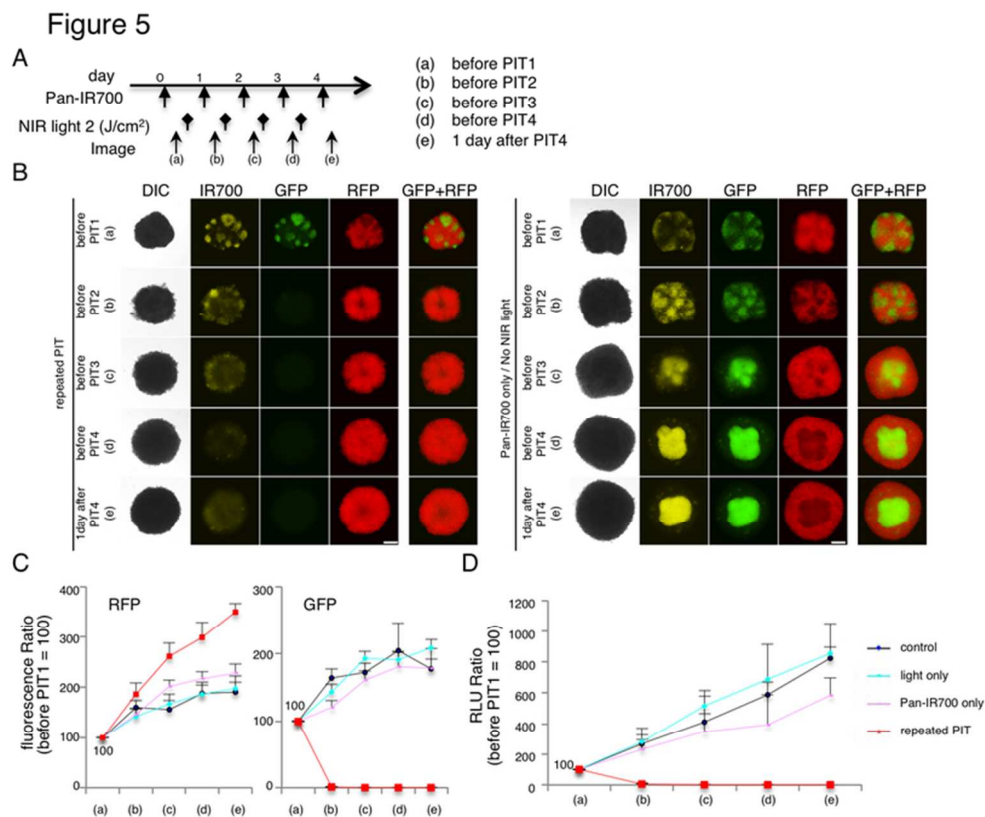
70x80mm (300 x 300 DPI)



Target cell elimination in 2D cell culture.

(A) Mixture of A431-luc-GFP cells and Balb/3T3-RFP cells were incubated with Pan-IR700 for 6 hr. Baseline and 1 hour post-APC with NIR light (2 J/cm²) microscopic images demonstrate specific cell killing of A431-luc-GFP. Bar = 20 μm. Membrane damage and necrosis induced by APC with NIR light was confirmed by dead cell Cytosine staining. Representative image demonstrates that A431-luc-GFP cells were eliminated 1hr after APC with NIR light exposure. Bar = 200 μm. (B) An almost confluent mixed cell culture of A431-luc-GFP and Balb/3T3-RFP was used. Cells were incubated with Pan-IR700 for 6 hr, and observed before and after irradiation with NIR light (2 J/cm²). (C) Repeated NIR-PIT (2 J/cm²) regimen is shown (2 J/cm²). (D) Repeated APC with NIR light completely eliminated targeted cells with no harm to non-targeted cells, until non-target cells became confluent. 100:10 ratio mixtures of A431-luc-GFP and Balb/3T3-RFP cells were cultured (other groups are in Figure S4C). Bar = 200 μm. (E) Quantification of fluorescence ratios showed complete elimination of targeted cells and no effect on non-targeted cells. (n = 10 fields in each group) (F) Quantification of luciferase activities (RLU ratio) demonstrates complete target cell elimination (n = 10 in each group). BLI was in Figure S4D.

70x80mm (300 x 300 DPI)

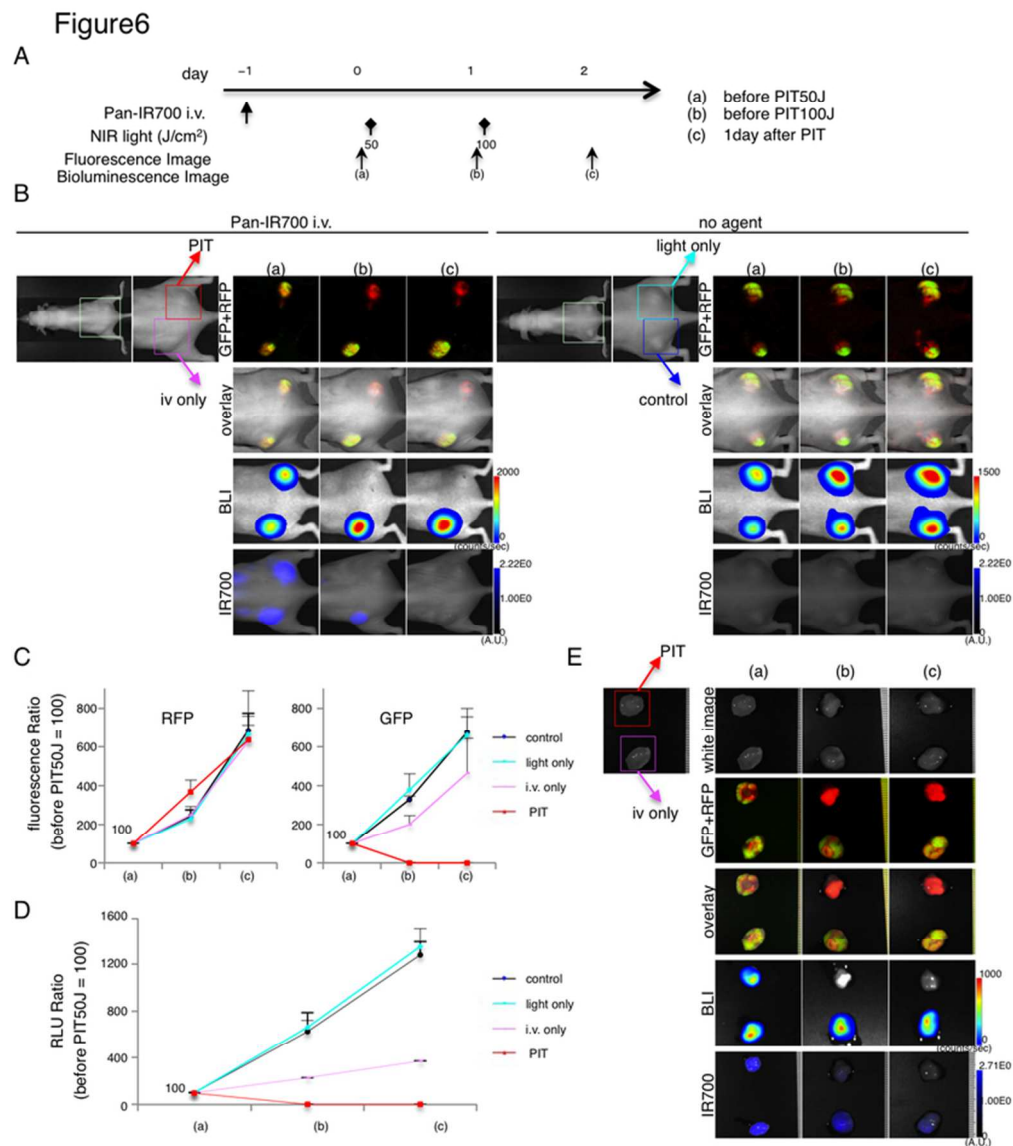


Target cell elimination in 3D spheroids ex vivo.

(A) NIR-PIT (2 J/cm²) regimen is shown. (B) Repeated APC with NIR light completely eliminated target cells with no harm to non-target cells, in a mixed 3D spheroid (other groups are in Figure S5D). Bar = 200 μ m.

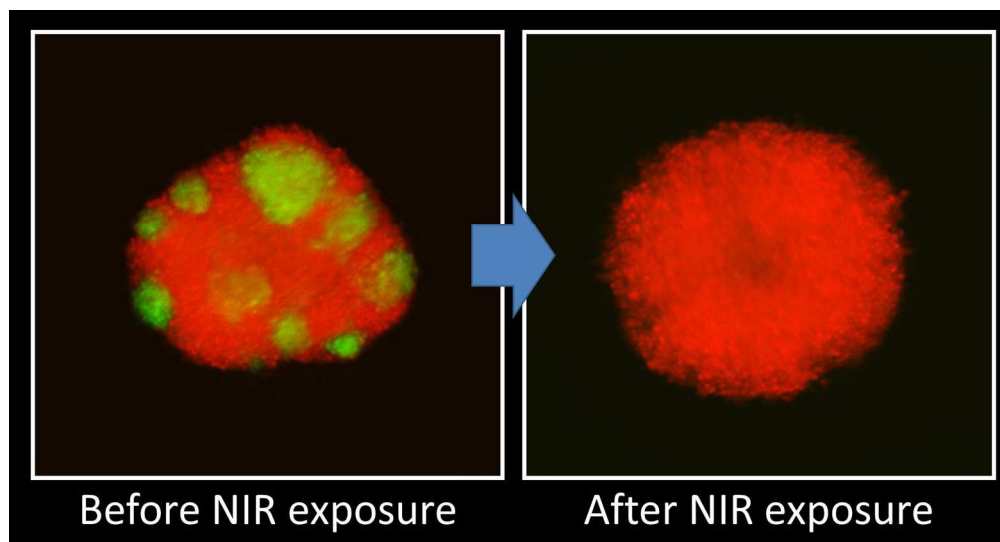
(C) Quantification of fluorescence ratios showed complete elimination of target cells and no effect on non-target cells. (n = 10 spheroids in each group) (D) Quantification of luciferase activities (RLU ratio) demonstrated complete elimination of target cells (n = 10 spheroids in each group). BLI and IR700 fluorescence images were in Figure S5E.

70x80mm (300 x 300 DPI)



Target cell elimination within mixed cell tumors in vivo.

(A) APC with NIR light ($2 J/cm^2$) regimen is shown. (B) Repeated APC with NIR light exposure completely eliminated target cells from mixed tumors in vivo. (C) Quantification of fluorescence ratios showed complete elimination of target cells in mixed tumors (Additional two mice images were in Figure S6C) ($n = 10$ in each group). (D) Quantification of luciferase activities (RLU ratio) demonstrated complete elimination of target cells in vivo. ($n = 10$ in each group). (E) Representative image of ex vivo tumors showed complete elimination of target cells from mixed tumors. Control was presented in Figure S6E. 70x80mm (300 x 300 DPI)



Before and after eliminating EGFR+ cells
199x106mm (300 x 300 DPI)